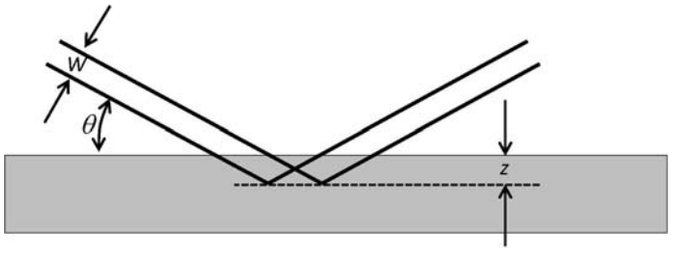

Figure 3.2.2
Sketch illustrating symmetrical diffraction from a flat sample.

Assume that the detector is large enough in the equatorial direction that all diffracted radiation is captured (*i.e.*, no loss of signal due to parallax). Radiation scattered from a volume element a distance z below the surface of the sample will have a total path length $2z/\sin\theta$; integration yields an effective sample volume of $WH/2\mu$, independent of diffraction angle. The situation is more complicated if a flat sample is not optically deep or if the sample is shorter than $W/\sin\theta$; in either case, computation of the effective volume is straightforward, as long as the sample geometry is known with sufficient accuracy. The calculations are described in detail in Chapter 5.4 of this volume.

Another important case is that of a cylindrical sample, such as a Lindemann capillary for X-rays or a can of appropriate material (often vanadium) for neutrons. The integration for $V_{\rm eff}$ above is given in convenient form for computation by Ida (2010), and is tabulated in *International Tables for Crystallography*, Volume C, Section 6.3.3.2. In the case of monochromatic radiation (neutrons or X-rays), for a given absorption constant μ, $V_{\rm eff}$ is an increasing function of diffraction angle 2θ so that higher-angle peaks will appear relatively stronger. Weak-to-moderate absorption from a cylindrical sample affects the observed intensities in essentially the same algebraic form as a negative effective Debye–Waller factor (Hewat, 1979), leading to significantly underestimated (perhaps even negative) measured Debye–Waller factors. In the case of pulsed neutrons, the effect is compounded by the fact that the absorption cross section is generally inversely proportional to the neutron velocity; consequently, in a given detector, faster neutrons, representing larger $|\mathbf{G}|$, will suffer less attenuation in the sample.

3.2.3.2. *Absorption with multiphase samples*

One important application of powder diffraction is the quantitative analysis of mixtures. Quantitative phase analysis is covered in detail in Chapter 3.9 of this volume; here we set the stage. If a sample is a mixture of several phases, the powder-diffraction pattern will be the sum of the patterns of each phase, weighted by the fraction of the illuminated volume occupied by that phase. The most common configuration for quantitative analysis by X-ray diffraction is reflection from an optically deep flat-plate sample. In this case, the integrated intensity of a particular reflection from the jth phase is

$$I_{hkl}(j) = I_0 LP(\theta)\frac{m_{hkl}(j)|A_{hkl}(j)|^2}{V^2(j)}\frac{w_m(j)}{\rho(j)\overline{\mu}}, \qquad (3.2.16)$$

where $V(j)$, $w_m(j)$ and $\rho(j)$ are the unit-cell volumes, mass fraction and density of phase j, respectively. Here I_0 is an overall intensity scale factor, $LP(\theta)$ is the Lorentz and polarization factor common to all phases, and $\bar{\mu} = \sum_j w_m(j)\mu(j)$ is the absorption coefficient of all solid phases in the sample. The summation includes all solid phases, even amorphous materials.

Note that the intensity of peaks from a particular phase is not simply proportional to the fraction of that phase present. For example, if there are two phases A and B, the intensity of A peaks will be proportional to

$$\frac{w_m(A)}{w_m(A)[\mu(A)-\mu(B)]+\mu(B)}.$$

3.2.3.3. *Granularity, microabsorption and surface roughness*

The above discussion of absorption in a powder sample is premised on the assumption that the powder sample is sufficiently fine that the beam traverses a large number of grains, *i.e.*, that $\mu\ell \ll 1$, where μ is the absorption coefficient in the solid material and ℓ is a characteristic linear grain dimension. In that case, the effective linear absorption constant is $\bar{\mu} = \mu\rho_{\rm powder}/\rho_{\rm solid}$, independent of the path that the radiation follows through the sample. However, if $\mu\ell$ is not very small, the simple picture of an average absorption length in the sample breaks down, leading to changes in the diffracted intensity.

There have been several treatments of microabsorption due to porosity and surface roughness. Rather than reviewing the literature, this section summarizes work of Hermann & Ermrich (1987) on a flat sample in the symmetrical reflection geometry discussed above. The single-phase sample is taken to be a collection of random polyhedra of average chord length ℓ with packing fraction α_0. The surface has the same lateral correlation length, but the average packing fraction rises from zero at the surface with characteristic dimension t_s, *i.e.*, $\alpha(z) = \alpha_0[1-\exp(-z/t_s)]$, where z is the distance from the surface into the sample. $t_s = 0$ represents an abrupt termination of the bulk porous material.

Hermann & Ermrich find that the diffracted intensity is reduced from the fine powder limit by a factor of $1 - P_{\rm bulk} - P_{\rm surface}$, where

$$P_{\rm bulk} \simeq 2\mu\ell(1-\alpha_0)^2,$$
$$P_{\rm surface} \simeq \frac{2\mu\alpha_0 t_s}{\sin\theta}\left(1-\frac{t_s}{\ell(1-\alpha_0)\sin\theta}\right).$$

If surface roughness is small, there is no dependence on diffraction angle 2θ, and the only effect is an overall reduction of diffracted intensity. Excess surface roughness ($t_s > 0$), as might be produced by allowing a granular powder to settle against a flat surface, leads to additional diminution of diffracted intensity at low angles. The expression for $P_{\rm surface}$ given above is to leading order in $1/\sin\theta$, and is therefore not valid for small grazing angles of incidence. Note that both the surface and bulk correction factors approach zero as $\mu\ell \to 0$. This analysis is in general agreement with analysis and measurements performed by Suortti (1972).

An additional effect of microabsorption in multi-component powders has been considered by Brindley (1945). The principle is illustrated in Fig. 3.2.3. An X-ray propagating through the sample (depicted by the broken line) suffers absorption according to the weighted average $\bar{\mu}$, but an X-ray diffracted in a grain of phase a has travelled further in that phase than average (solid line). If its path in the diffracting grain is x and the total path through the sample is L, absorption will reduce its intensity by a factor

$$\exp(-\mu_a x)\exp[-\overline{\mu}(L-x)].$$

Copyright © 2018 International Union of Crystallography

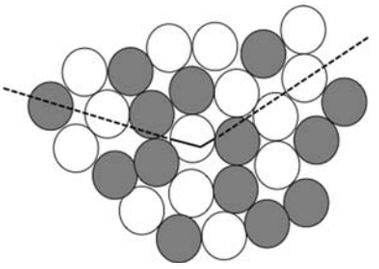

Figure 3.2.3
Sketch illustrating an X-ray propagating through a mixture of two kinds of particles.

This leads to a weaker observed reflection from a phase a with larger absorption constant μ_a if the particle size is an appreciable fraction of $1/(\mu_a - \bar{\mu})$.

Averaging over the particle volume, we see that the observed intensity of phase a will be lowered from its value in a fine powder by a factor

$$\tau = V_a^{-1} \int \exp[-(\mu_a - \overline{\mu})x]\, \mathrm{d}V_a,$$

where the integral is taken over one representative grain of phase a. This is exactly the integral of equation (3.2.15), and if one assumes monodisperse spherical particles, it is tabulated in *International Tables for Crystallography*, Volume C, Section 6.3.3.2 and elsewhere, with $\mu_a - \bar{\mu}$ replacing μ. One hitch is that the tabulations are for $\mu > 0$, whereas $\mu_a - \bar{\mu} < 0$ for the less absorbing phases in a mixture. Brindley handles this with a series expansion and provides a table of τ *versus* $(\mu_a - \bar{\mu})R$.

By way of illustration, consider a mixture of equal weight fractions of corundum, magnetite and zircon powders, analysed with Cu $K\alpha$ radiation. Fig. 3.2.4 shows the weight fractions that would be measured from such a sample as a function of particle radius (assumed equal for all three phases). In this case, microabsorption biases the result by about 10% for particles of 10 μm diameter, and misses by a factor of two if the diameter is 70 μm.

In considering microabsorption, there are several important points to note. This entire analysis is only valid for $\mu R \ll 1$, since otherwise the concept of an average absorption length becomes ill defined. That means that the Brindley analysis breaks down precisely when it becomes significant. Of course, the Brindley assumption of monodisperse spherical particles is unrealistic for most real samples. Both the surface roughness and Brindley corrections depend on diffraction angle as well as μR, but, as noted above, for moderate absorption, the angle dependence appears as an effective Debye–Waller factor. The parameter R is the radius of the grain of material, which is commonly very much larger than the size of a coherently diffracting region; a Scherrer analysis of particle size through line broadening does not provide a useful estimate of R. Most importantly, unless one has an accurate independent measurement of the size and shape of the grains, microabsorption corrections should be taken as a sign of impending trouble, not a quantitative correction.

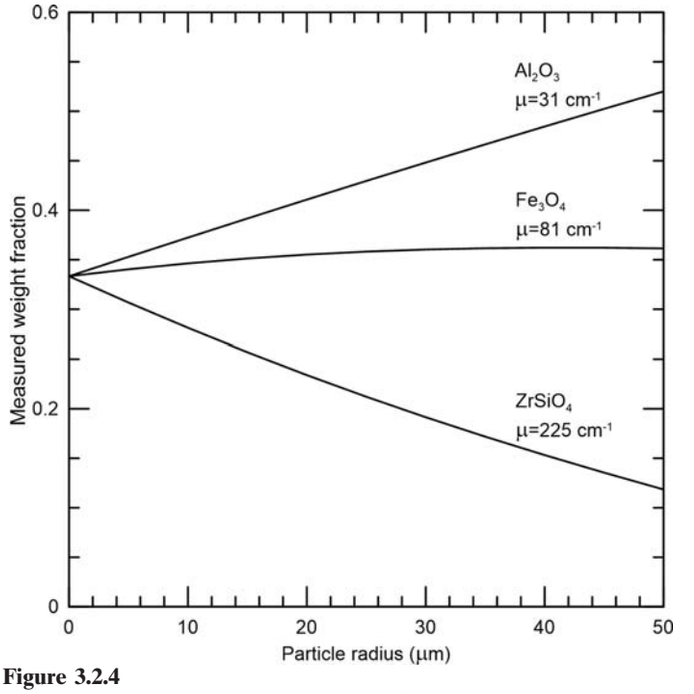

Figure 3.2.4
Weight fractions that would be measured from a mixture of equal parts of three phases with Cu $K\alpha$ radiation.

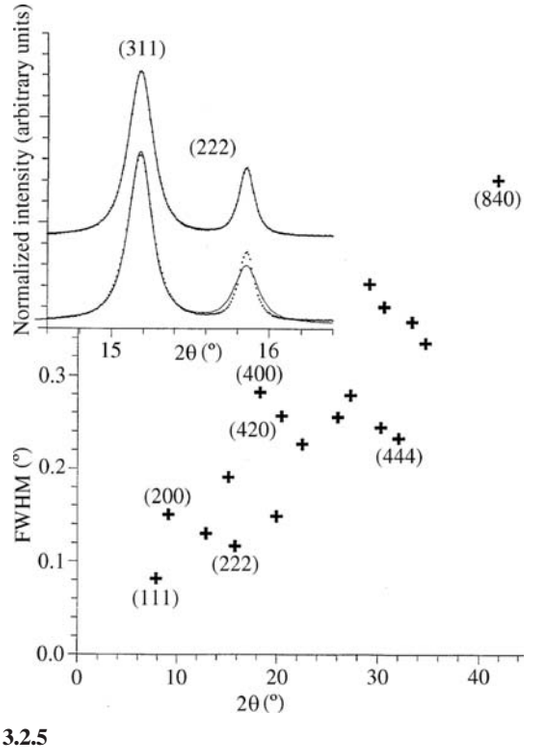

Figure 3.2.5
Diffraction peak width *versus* diffraction angle from a powder pattern of face-centred cubic Rb_3C_{60} (Stephens, 1999). The inset at the top shows a limited range of the data, fitted by a model with two different peak widths (upper trace) and with the widths constrained to be equal (lower trace).

3.2.3.4. *Anisotropic strain broadening*

Strain broadening is often observed not to be monotonically dependent on the magnitude of the d-spacing, but to have a more complicated dependence on the direction of the diffraction vector **G**. An illustration of the effect in cubic Rb_3C_{60} is shown in Fig. 3.2.5 (Stephens, 1999). The lower part of the figure shows an apparently irregular trend of diffraction peak widths on diffraction angle 2θ.

Whatever the nature of random internal stresses and strains, it can be argued on general grounds that strain broadening depends on a combination of fourth-rank tensors. On the assumption that the distribution of random strains is Gaussian, each diffraction peak has Gaussian shape, and the variance of the inverse d-spacing squared is a quartic form in the reflection indices (hkl). This can be expressed as

references